Complexity Project: The Oslo Model

CID: 01531221

22nd February 2021

Abstract

This report presents an investigation of the Oslo Model; one of the simplest models displaying self-organised criticality. Initially, the Oslo Model was built using Python and was tested to ensure the algorithm works as intended. Then, the height of the system was investigated to explore its scaling with system size and any signs of corrections to scaling. A data collapse was produced for the height of the system to understand how it behaves in transient and recurrent configurations, while a data collapse for the height probabilities in the steady state was produced to understand its underlying statistics. Finally, to demonstrate fundamental aspects of self-organised criticality – scaling and data collapse – the critical exponents of the Oslo Model were determined by performing a data collapse and by applying the moment analysis of the avalanche-size probabilities. It was found that the height scales linearly with the system size, while the time to reach steady state scales by the square of the system size. It was also found using an algebraic and a geometric argument that the transient state relates to the square of the number of grains added to the system, while the data collapse for the height probabilities demonstrated that the slopes of the system are dependent random variables and do not follow a normal distribution. Finally, the system was found to have no typical avalanche size, while the critical exponents were determined to be $D = 2.086 \pm 0.008$ and $\tau_s = 1.52 \pm 0.01$ using k'th moment analysis, demonstrating that the system is consistent with the framework for data collapse and finite-size scaling.

Word Count: 2,486

1 Introduction

Various systems consist of many interacting parts whose interaction exhibits macroscopic phenomena, like thermodynamic properties of gases arising from the collisions and interactions of individual gas particles. The connection between these macroscopic phenomena and their underlying processes is explored using the Oslo Model, understanding how self-organised criticality is displayed in such systems. The Oslo Model was explored to investigate whether it spontaneously reaches a steady state and whether that state is an attractor of the dynamics of the system, while its response to small perturbations – avalanches – were observed to see if they exhibit scale-free behaviour. The sections below outline the topics investigated to ultimately show that the Oslo Model is consistent with the framework for data collapse and finite-size scaling.

Outline

2 Oslo Model

We consider a $d = 1$ lattice of L sites, $i = 1, 2, ..., L$ with heights h_i slopes z_i, and threshold slopes z_i^{th} for each site i.

2.1 Algorithm

The Oslo Model algorithm consists of 3 parts:

1. **Drive:** add one grain at the first site of the lattice $i = 1$
2. **Relaxation:** relax supercritical sites – all sites where the slope is above the threshold slope, until $z_i \leq z_i^{th}\ \forall i$, then re-assign the threshold slopes of all relaxed sites: $z_i^{th} \in \{1, 2\}$ with probability p for 1 and $1 - p$ for 2
3. **Iteration:** return to **1**

For the Oslo Model we set $p = 0.5$. The size of an avalanche s is defined as the total number of relaxations caused by the addition of one grain, including $s = 0$.

2.2 Testing the Model

To ensure the algorithm works as intended we need to check its main rule: all supercritical sites are correctly relaxed, as shown in Figure 2.1.

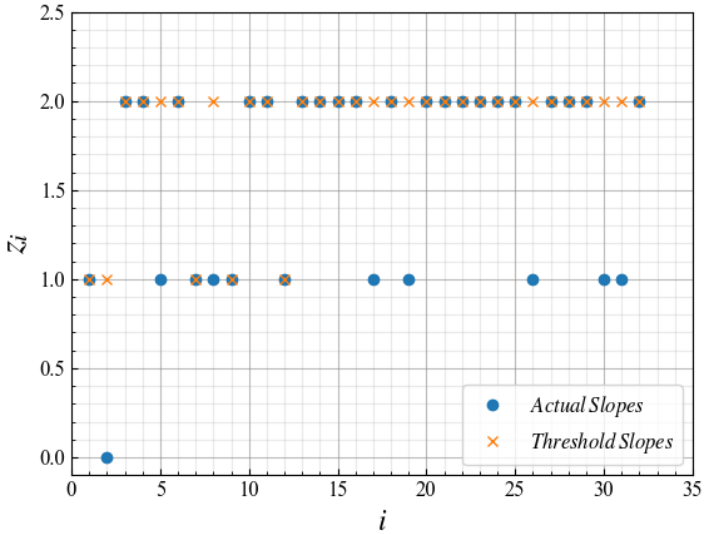

Fig. 2.1 The actual slopes (blue dots) and the threshold slopes (orange crosses) in a stable configuration for a system of size $L = 32$. All slopes are bounded by their respective threshold slopes, thus demonstrating that $z_i \leq z_i^{th}\ \forall i$, as expected in a stable configuration.

To check that the system is driven and relaxed appropriately at all sites, we can verify that the average steady-state height of the pile is 26.5 and 53.9 for $L = 16$ and $L = 32$ respectively [1], as shown in Figure 2.2(a), where the height of the pile after having added t grains is

$$h(t; L) = \sum_{i=1}^{L} z_i(t). \tag{1}$$

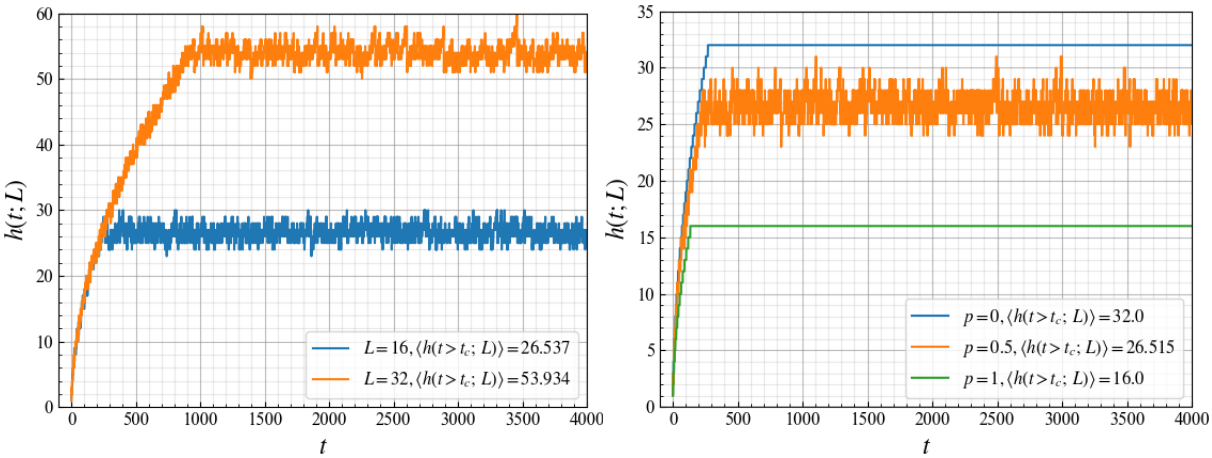

Fig. 2.2 (a) The height of the pile $h(t; L)$ against time t (in units of added grains) for $L = 16$ (blue) and $L = 32$ (orange), with average steady-state heights of $26.537 \approx 26.5$ and $53.934 \approx 53.9$ respectively, as expected [1]. (b) The height of the pile $h(t; L)$ against time t for $L = 16$, with $p = 0$ (blue), $p = 0.5$ (orange) and $p = 1$ (green), with respective average steady-state heights of 32.0, 26.515 and 16.0.

Since $p = 0.5$ for the Oslo Model one would expect the slopes z_i to be uniformly distributed, thus the average slope being 1.5. However, Figure 2.2(a) demonstrates that the average slope is 1.659 for $L = 16$ and 1.685 for $L = 32$. This occurs because threshold slopes of 2 last longer than threshold slopes of 1 as it takes an additional grain to reach that. Slopes of 2 are thus reset less often, increasing their appearance, hence, z_i are not uniformly distributed.

Moreover, we can ensure that the algorithm works properly by changing the probability of choosing a threshold slope of 1, as shown in Figure 2.2(b). If we set $p = 0$, all slopes are always 2, thus the steady-state height for $L = 16$ is precisely 32 and does not vary, while conversely, if we set $p = 1$, all slopes are always 1 and the steady-state height is precisely 16, as expected.

We can also verify that the algorithm works correctly by counting the total number of recurrent configurations. Running the model for $L = 2$ and $L = 4$ (main.py, line: 1283) returns a total of 5 and 34 recurrent configurations respectively, as expected [2]. Finally, as will be investigated later, we can check that $\langle s \rangle \propto L$ [2], shown in Figure 2.3.

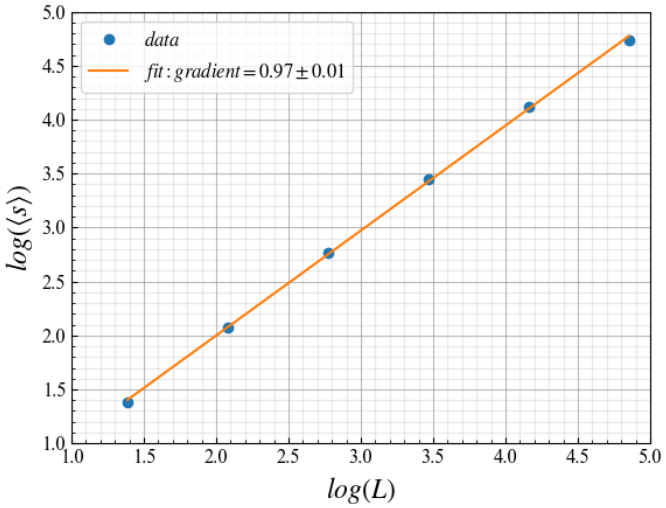

Fig. 2.3 Double logarithmic plot of the average avalanche size $\langle s \rangle$ against the system size L (blue dots). A linear fit (orange) has gradient of 0.973 ± 0.01 representing the exponent of L, which is approximately 1, demonstrates that $\langle s \rangle$ scales linearly with L, as expected, indicating that the model works as intended.

3 Pile Height $h(t; L)$

3.1 Transient and Recurrent Configurations

To investigate transient and recurrent configurations we can plot the height of the pile, starting from empty systems for different system sizes, as shown in Figure 3.1.

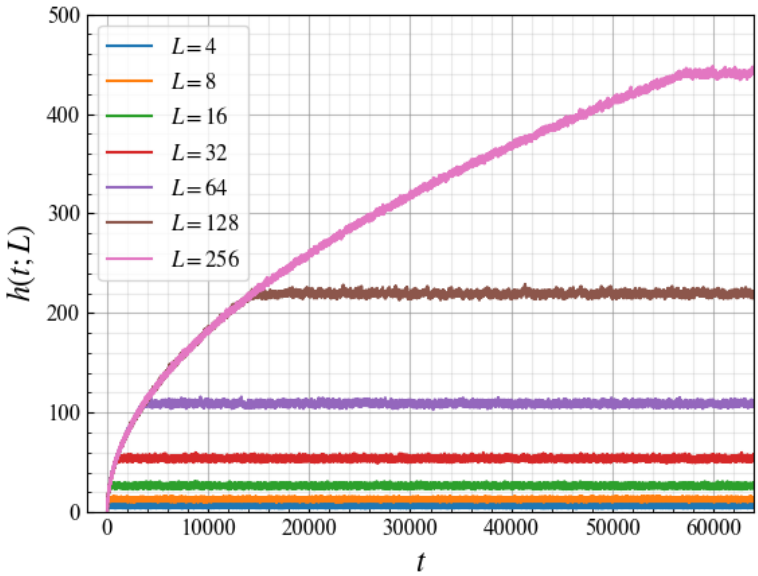

Fig. 3.1 Total height $h(t; L)$ of the pile against time t, starting from an empty set for different system sizes.

Figure 3.1 shows that all transient states superpose for all L, demonstrating that the system is 'unaware' of its size until it reaches the steady state. As a result, the transient state is independent of L and the pile builds up the same way for all system sizes. The

indefinitely revisited recurrent configurations comprise the horizontal parts of the plot, where the height oscillates about its statistically stationary average steady-state height.

3.2 Scaling of Averaged Cross-Over Time $\langle t_c(L)\rangle$

The time just before the first grain leaves the system is defined as the cross-over time, equivalent to the number of grains in the system at that time. The scaling of the averaged cross-over time $\langle t_c(L)\rangle$ with L obtained by a double-logarithmic plot shown in Figure 3.2, is $\langle t_c(L)\rangle \propto L^2$.

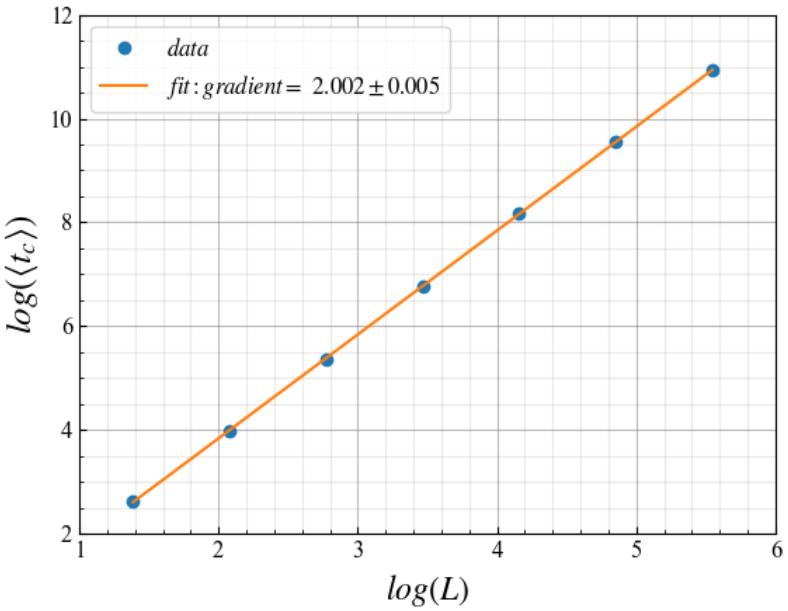

Fig. 3.2 Double logarithmic plot of the averaged cross-over time $\langle t_c(L)\rangle$ against the system size L (blue dots). A linear fit has gradient of 2.002 ± 0.005 representing the exponent of L, which is approximately 2, demonstrating that $\langle t_c(L)\rangle \propto L^2$.

3.3 Theoretical Argument for Scaling of $h(t;L)$ and $\langle t_c(L)\rangle$

To understand how $h(t;L)$ scales with L for $L \gg 1$, we can think of the system as a right-angled triangle.

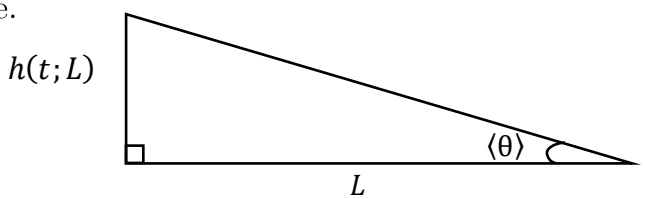

Fig. 3.3 System in steady state, simplified for $L \gg 1$ as a right-angled triangle of base L, height $h(t;L)$ and angle $\langle\theta\rangle$, that is, the average angle.

Since we ignore corrections to scaling for $L \gg 1$, then:

$$h(t;L) = tan(\langle\theta\rangle)\, L \equiv \langle slope\rangle\, L, \tag{2}$$

thus, $h(t;L)$ scales linearly with L.

The cross-over time is the number of grains in the system before the first grain leaves the system, thus relating to the area of the triangle, $A = \frac{1}{2} * base * height$:

$$\langle t_c(L) \rangle \propto \frac{1}{2} * h(t;L) * L = \frac{1}{2} * \langle slope \rangle L * L = \frac{1}{2} L^2. \quad (3)$$

Therefore, $\langle t_c(L) \rangle \propto L^2$. A similar scaling is obtained by considering the cross-over time as proportional to the sum of the heights:

$$\langle t_c(L) \rangle = c \sum_{i=1}^{L} h_i = c \frac{L(L+1)}{2} = c \left(\frac{L^2}{2} + \frac{L}{2} \right) \sim c \frac{L^2}{2} \quad for\ L \gg 1, \quad (4)$$

where c is a constant relating to the number of grains per unit square. Moreover, we know that the minimum bound for $\langle t_c(L) \rangle$ is $c \left(\frac{L^2}{2} + \frac{L}{2} \right)$ with a minimum $\langle slope \rangle$ of 1, and the maximum bound for $\langle t_c(L) \rangle$ is $2c \left(\frac{L^2}{2} + \frac{L}{2} \right)$ with a maximum $\langle slope \rangle$ of 2, thus $c \left(\frac{L^2}{2} + \frac{L}{2} \right) \leq \langle t_c(L) \rangle \leq 2c \left(\frac{L^2}{2} + \frac{L}{2} \right)$, so $\langle t_c(L) \rangle$ definitely scales as L^2 for $L \gg 1$.

3.4 Data Collapse of Averaged Height $\tilde{h}(t;L)$

Using the scaling relations of $h(t;L)$ and $\langle t_c(L) \rangle$ we can produce a data collapse for the heights shown in Figure 3.4, introducing a scaling function for $h(t;L)$.

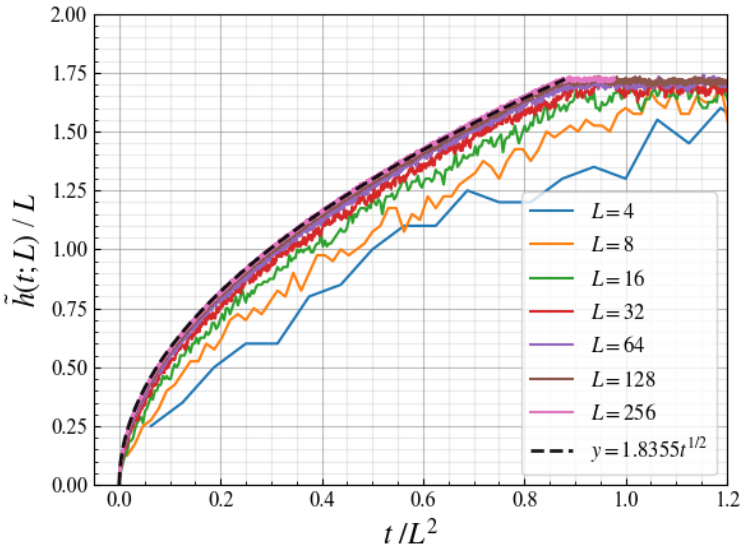

Fig. 3.4 Data collapse for the processed heights $\tilde{h}(t;L) = \frac{1}{M} \sum_{j=1}^{M} h^j(t;L)$, where $M = 6$ realisations of the system. The transient state (black dotted line) is $y = 1.8355t^{1/2}$.

To collapse the heights and show their critical behaviour we want to introduce a scaling function of one variable only. As $\tilde{h}(t;L) \propto L$, we can divide it by L, and as $\langle t_c(L) \rangle \propto L^2$, we can divide t by L^2. As a result, $\tilde{h}(t;L) = LF(t/L^2) \equiv LF(x)$, where $x = t/L^2$.

When $x \gg 1$ then $t \gg L^2$, thus, the system is in steady-state and F becomes a constant, as the system stops growing and is statistically stationary, $\langle added\ grains \rangle \equiv \langle grains\ leaving \rangle$, shown by the horizontal section of Figure 3.4. When $x \ll 1$, then $t \ll L^2$, or $t \to 0$, thus, the system is in transient state. Since we know that the transient state is independent of L, we want $\tilde{h}(t; L) = \tilde{h}(t)$. To achieve that, $F := \frac{g(t)}{L}$ so that $\tilde{h}(t; L) = g(t)$. The only functional form $g(t)$ can take so that $F = F\left(\frac{t}{L^2}\right) = \frac{g(t)}{L}$ is $g(t) = \sqrt{t}$, thus, $\tilde{h}(t) \propto \sqrt{t}$. This can also be stated geometrically: at time t the fraction of the total volume filled up $\propto \frac{t}{L^2}$, and for a $2D$ object the fraction of the total height at time t is the square root of the volume, $\frac{\tilde{h}(t;L)}{L} \propto \sqrt{t/L^2}$ thus, $\tilde{h}(t;\ L) \propto \sqrt{t}$.

3.5 Corrections to Scaling of Average Height $\langle h(t; L) \rangle_t$

To investigate whether the average height in the steady-state contains any signs of correction to scaling we assume:

$$\langle h(t; L) \rangle_t = a_0 L(1 - a_1 L^{-\omega_1} + a_2 L^{-\omega_2} + \cdots), \qquad (5)[1]$$

where $\omega_i > 0$ and a_i are constants. We can obtain a_0 by considering only the leading term of L for $L \gg 1$, such that $a_0 = \frac{\langle h(t;L) \rangle_t}{L}$. Using our highest L, $L = 256$, $a_0 = 1.723$. As a_0 is known, we can rearrange Eqn. (5) into Eqn. (6), neglecting terms where $i > 1$:

$$log\left(L - \frac{\langle h(t;L) \rangle_t}{a_0}\right) = (1 - \omega_1) log(L) + log(a_1), \qquad (6)$$

and obtain ω_1 from the gradient of Eqn. (6) for small L, shown in Figure 3.5.

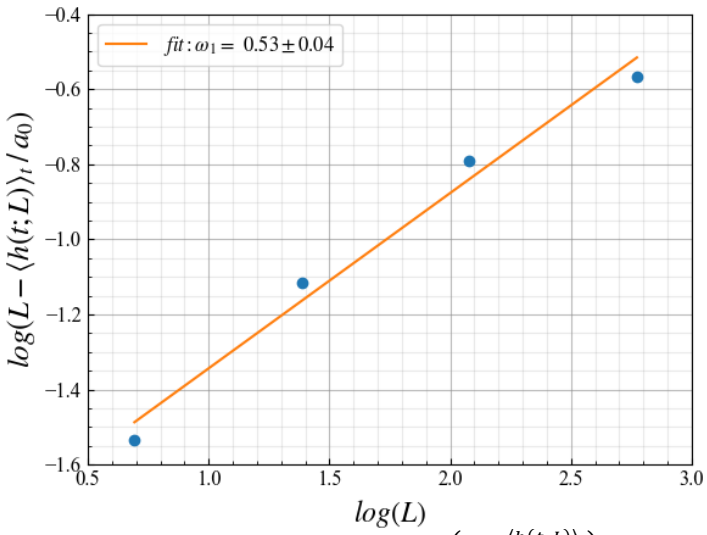

Fig. 3.5 Double-logarithmic plot of $\left(L - \frac{\langle h(t;L) \rangle_t}{a_0}\right)$ against L (blue dots). A linear fit (orange) with $gradient = 1 - \omega_1 = 0.47 \pm 0.04$, thus, $\omega_1 = 0.53 \pm 0.04$.

This procedure of using large L to obtain a_0 and small L to obtain ω_1, where corrections to scaling have a larger impact on $\langle h(t; L) \rangle_t$, converges to the actual values

of $\langle h(t;L)\rangle_t$ for small L better than a fitted curve using Scipy's curve-fitting algorithm, shown in Figure 3.6.

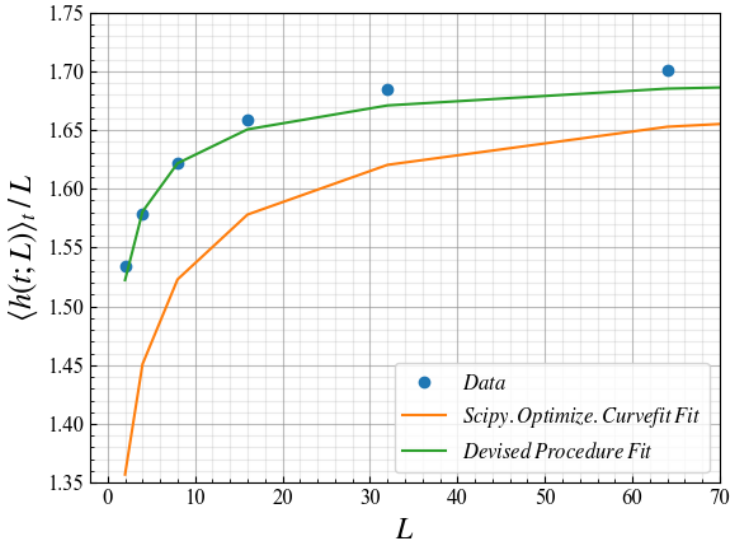

Fig. 3.6 Data for $\langle h(t;L)\rangle_t/L$ plotted against L (blue dots), curve fit using Scipy's Optimize.Curvefit (orange), curve fit using the devised procedure detailed above (green). Corrections to scaling have a larger impact on small L, from which ω_1 was obtained. Main deviation of Scipy's curve-fit originates from its error in estimating a_1, while the true points lie outside the range of uncertainties of ω_1 and a_1.

3.6 Scaling of Standard Deviation $\sigma_h(L)$

To obtain the scaling of $\sigma_h(L)$ with L we can plot them on a double-logarithmic plot, shown in Figure 3.7.

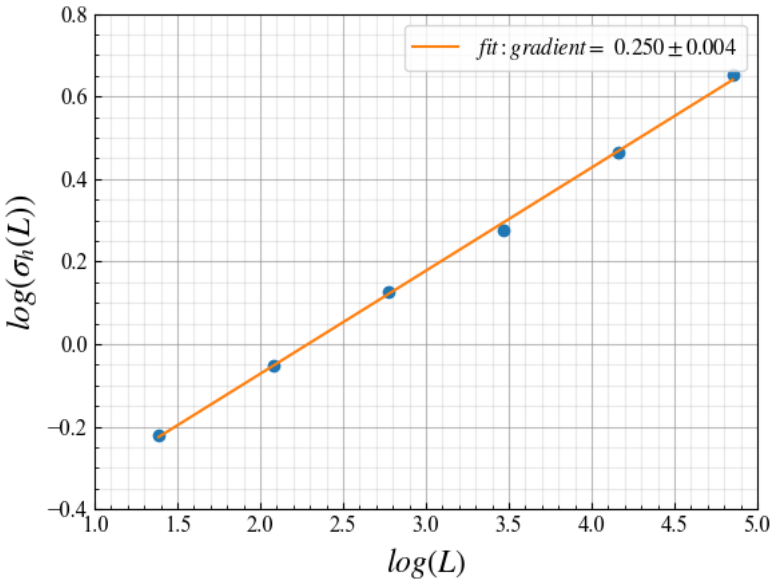

Fig. 3.7 Double logarithmic plot of the standard deviation $\sigma_h(L)$ against L (blue dots). A linear fit (orange) with gradient of 0.250 ± 0.004, representing the exponent of L, demonstrates that $\sigma_h(L) \propto L^{0.25}$. As a result, $\sigma_h(L) \to \infty$ as $L \to \infty$.

Therefore, as $L \to \infty$ the average slope of $\langle h(t;L)\rangle_t$ given by $\langle h(t;L)\rangle_t/L = a_0 - a_0a_1L^{-\omega_1} + a_0a_2L^{-\omega_2}$ tends to a_0, as all terms of L tend to zero, while $\sigma_h(L) \to \infty$ as

$\sigma_h(L) \propto L^{0.25}$, demonstrating that corrections to scaling vanish for very large L, while $\langle h(t;L)\rangle_t$ can vary infinitely with infinite L.

3.7 Height Probability $P(\mathrm{h};L)$ & Data Collapse

As stated in Eqn. (1), $h(t;L) = \sum_{i=1}^{L} z_i(t)$. If we assume that z_i are independent, identically distributed random variables with finite variance $\sigma_{z_i}^2$, then, we would expect the probability $P(h;L)$ of $h(t;L)$ to follow a normal distribution when $L \gg 1$, following from the Central Limit Theorem (CLT), as $h(t;L)$ represents the large sum of independent random variables. Using error propagation:

$$\sigma_h(L) = \sqrt{\sum_{i=1}^{L} \left(\frac{\partial h}{\partial z_i}\right)^2 \sigma_{z_i}^2}. \tag{7}$$

From Eqn. (1) $\frac{\partial h}{\partial z_i} = 1$, therefore:

$$\sigma_h(L) = \sqrt{\sum_{i=1}^{L} \sigma_{z_i}^2} = \sqrt{\sigma_z^2 \sum_{i=1}^{L} 1} = \sqrt{(L\sigma_z^2)} \equiv \sigma_z L^{1/2}, \tag{8}$$

as all σ_{z_i} are equivalent since z_i are identically distributed. Therefore, $\sigma_h(L) \propto L^{1/2}$, implying that the divergence of $\sigma_h(L)$ as $L \to \infty$ arises purely from L and not from σ_z. The obtained height probabilities for different system sizes are shown in Figure 3.8.

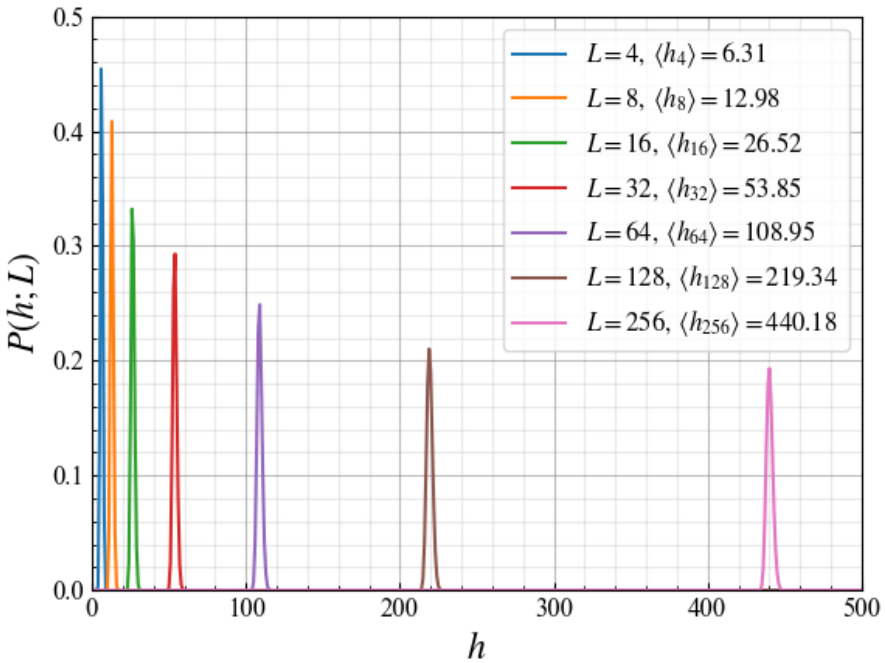

Fig. 3.8 Height probabilities $P(h;L) = \frac{\#observed\ configurations\ with\ h\ in\ pile\ of\ size\ L}{\#total\ observed\ configurations}$ against h for different system sizes.

If we assume that $P(h;L)$ is normal, we can produce a data collapse by stating that:

$$P(h;L) = \frac{1}{\sigma_h\sqrt{(2\pi)}}\ exp\left(-\frac{1}{2}\left(\frac{h-\langle h\rangle}{\sigma_h}\right)^2\right), \tag{9}$$

where $\langle h\rangle$ is the average height. Therefore, we can express Eqn. (9) to be scale-free:

$$\sigma_h P(h;L) = \frac{1}{\sqrt{(2\pi)}} exp\left(-\frac{1}{2}x^2\right), \tag{10}$$

where $x = \frac{h-\langle h\rangle}{\sigma_h}$. Eqn. (10) is now a function of one variable only, and if we plot $\sigma_h P(h;L)$ against x, we can collapse all the height probabilities together, shown in Figure 3.9.

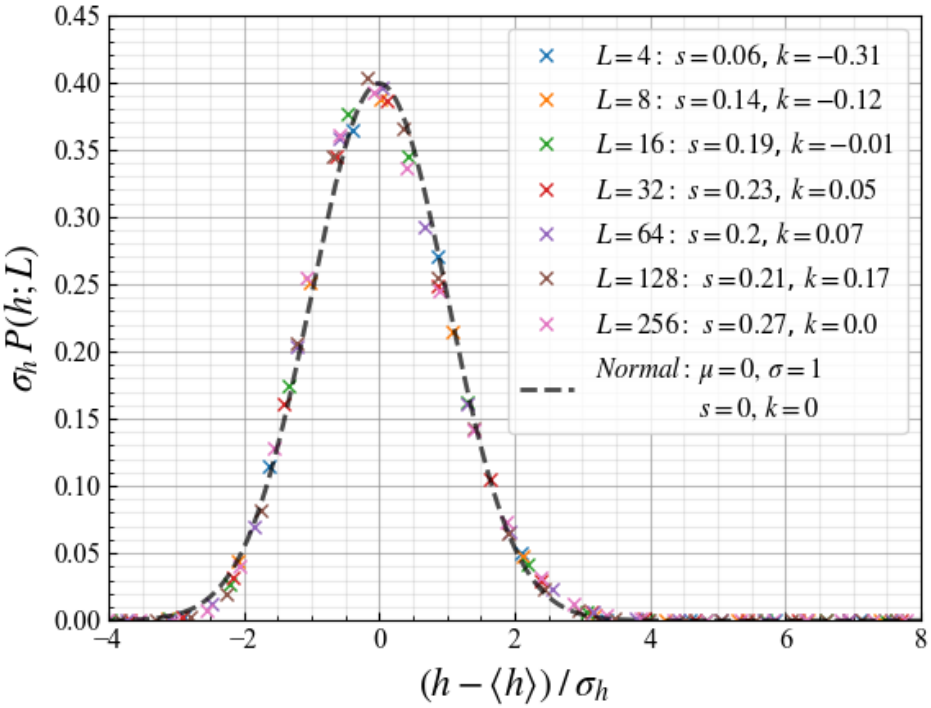

Fig. 3.9 Data collapse for the height probabilities (coloured crosses), plotting $\sigma_h P(h;L)$ against $\frac{h-\langle h\rangle}{\sigma_h}$, assuming that the height probabilities are normal. Normal PDF plotted in a black dotted line. The skewness of the data is indicated by s, while the kurtosis of the data is indicated by k.

From first inspection it appears that the heights are indeed distributed with a normal distribution. However, a small positive skew is visible on both tails of the distribution, indicated by s in Figure 3.9. The fact that there is a positive skew for all system sizes and that it grows with system size proves that the heights are not in fact normally distributed, negating the assumption that z_i are independent random variables, hence, the CLT does not apply. This stems from the definition of the Oslo Model, where toppling one grain changes its own slope, as well as that of its two adjacent sites,

enabling it to 'self-organise' itself. The positive skew is made more evident if the probabilities are plotted in a log-linear plot, shown in Figure 3.10.

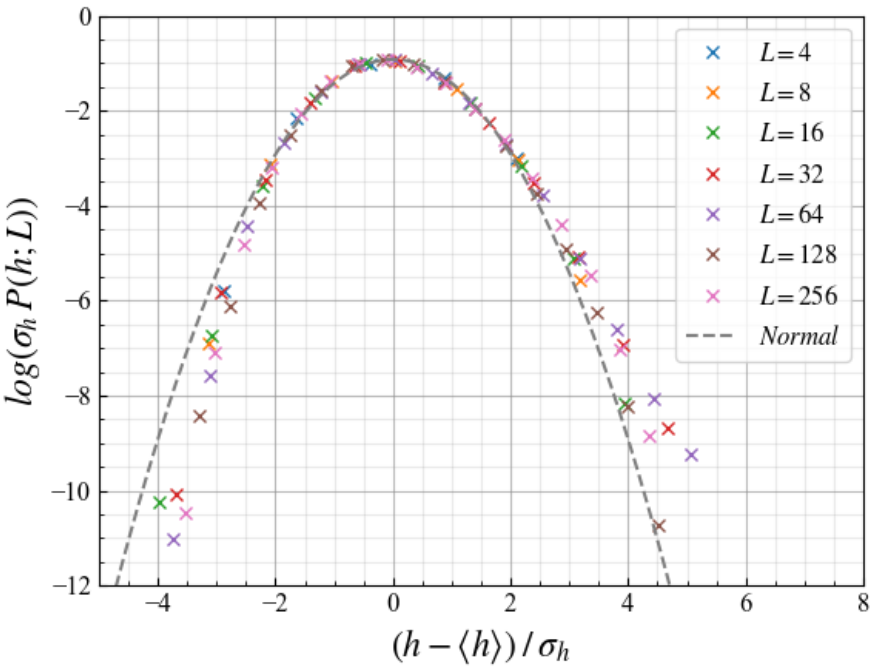

Fig. 3.10 Data collapse for the height probabilities (coloured crosses) in a log-linear plot, plotting $log(\sigma_h P(h;L))$ against $\frac{h-\langle h\rangle}{\sigma_h}$, as well as a normal PDF (grey dotted line). The positive skew on both tails of the distribution – a negative parabola in log-linear space – is now more evident, demonstrating that the height probabilities are not normal and that z_i are not independent.

4 Avalanche-Size Probability $P(s;L)$

Two methods, performing a data collapse and applying the moment analysis of the avalanche-size probability, are used to obtain the critical exponents D and τ_s of the Oslo Model, demonstrating criticality.

4.1 Avalanche-Size Probability and Finite-Size Scaling Ansatz

As described in ***2.1***, an avalanche size s is defined as the total number of relaxations caused by the addition of one grain, including $s = 0$, and we are only interested in avalanches occurring in the steady-state. As very large avalanches are very rare, there is very sparse statistics about them, inadequate to uncover a finite cut-off size s_c, thus introducing a noisy tail in the avalanche-size probabilities $P(s;L)$ for large s. To overcome this issue, we are using exponential increasing bins which can obtain information from the noisy tail of $P(s;L)$ where there is not enough statistics, and can

remove the noise for large s while approximating the actual $P(s;L)$ quite well, shown in Figure 4.1 for different system sizes.

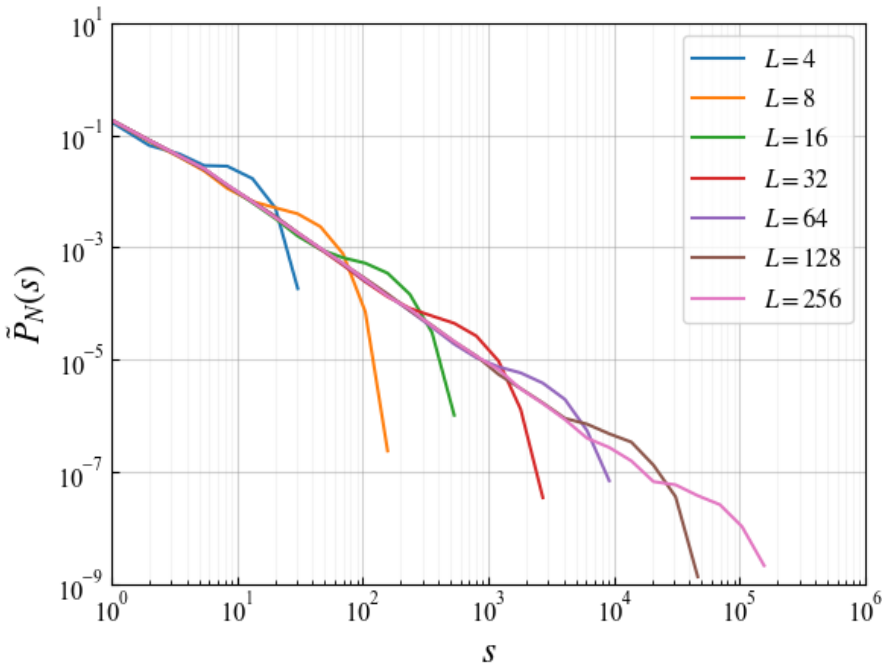

Fig. 4.1 Avalanche size probabilities $\tilde{P}_N(s;\ L)$ plotted against avalanche size s in a double-logarithmic scale, for different system sizes, for $N = 128{,}000$ samples in the steady state.

Figure 4.1 shows that the avalanche-size probability $P(s;L)$ can be well approximated by a power law, that is, $P(s;L) \propto s^{-\tau_s}$ for a scaling region: $1 \ll s \ll s_c(L)$. This demonstrates that there is no typical avalanche size, except for a maximum (cut-off) avalanche size that scales with L, $s_c(L) \propto L$, which is determined by the finiteness of the system. This shows that the avalanche sizes are bounded by the system, as there is a physical limit in the maximum number of grains that can leave the system. Moreover, there is a characteristic 'bump' in $P(s;L)$, where $P(s;L)$ is greater than some smaller and larger avalanche sizes, evidence of avalanches which ended prematurely as a consequence of the boundaries of the system [3].

We can then verify that $P(s;L)$ is consistent with the finite-size scaling ansatz

$$\tilde{P}_N(s;\ L) \propto s^{-\tau_s} G(s/L^D) \quad \text{for } L \gg 1,\ s \gg 1, \tag{11}$$

for which we first need to determine τ_s and D. To obtain τ_s we can assume Eqn. (11) and thus plot $log\left(\tilde{P}_N(s;\ L)\right)$ against $log(s)$ for the scaling region of Figure 4.1, where τ_s will be the negative of the gradient, shown in Figure 4.2(a). To obtain D we can plot $log(s_c)$ against $log(L)$, as we know that $s_c \propto L^D$ [2], shown in Figure 4.2(b).

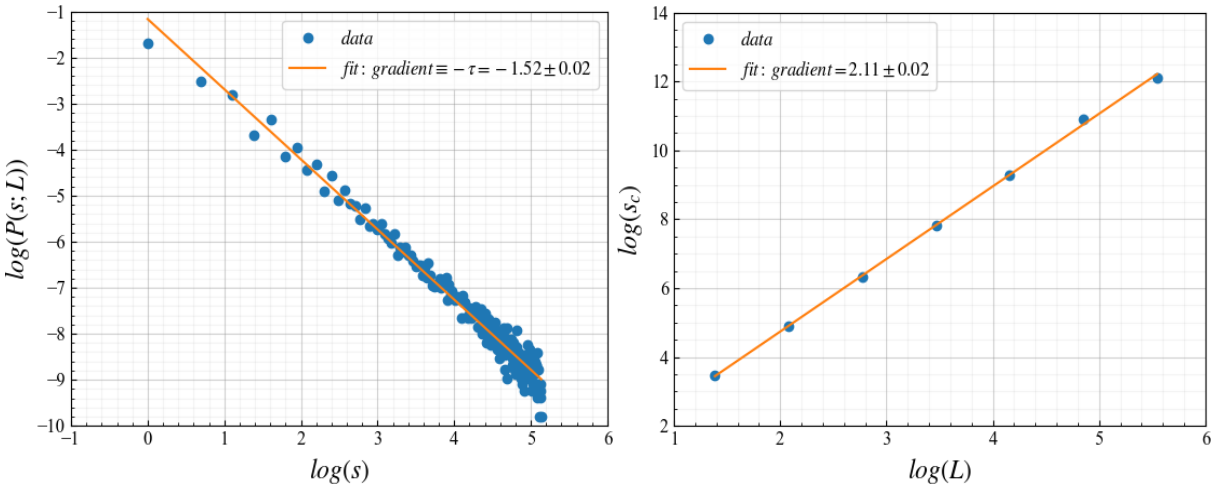

Fig. 4.2 (a) Double logarithmic plot of $P(s;L)$ against s (blue dots) in scaling region, for $L = 32$. A linear fit (orange) with gradient of -1.52 ± 0.02, representing $-\tau_s$, thus $\tau_s = 1.52 \pm 0.02$. (b) Double logarithmic plot of s_c against L (blue dots). A linear fit (orange) with gradient of 2.11 ± 0.02, which represents the exponent of L, thus $D = 2.11 \pm 0.02$.

The values of τ_s and D obtained, 1.52 and 2.11 respectively, are then used to collapse the avalanche-size probabilities, demonstrating that they are consistent with the finite-size scaling ansatz, shown in Figure 4.3.

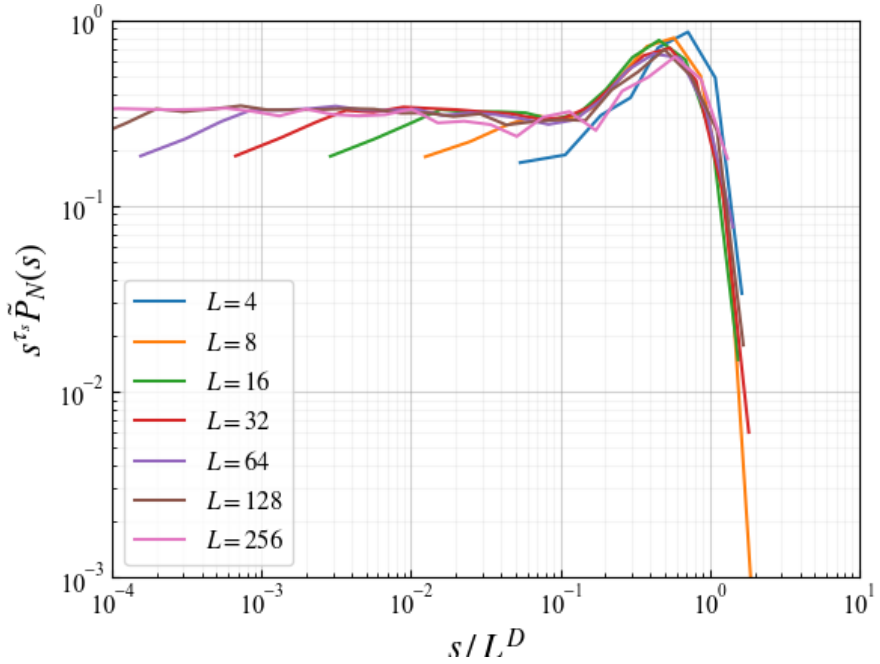

Fig. 4.3 Data collapse for the avalanche-size probabilities, using $D = 2.11$ and $\tau_s = 1.52$, plotting the transformed avalanche-size probability $s^{-\tau_s}P(s;L)$ against the rescaled avalanche size s/L^D. All curves have collapsed onto the scaling G for the Oslo Model, being consistent with the finite-size scaling ansatz.

To produce the data collapse, Eqn. (11) was re-arranged as $s^{\tau_s}\tilde{P}_N(s;\ L) \propto G(x)$, where $x = s/L^D$, and $s^{\tau_s}\tilde{P}_N(s;\ L)$ was plotted against x. All curves collapsed onto the scaling G for the Oslo Model, and the quality of the collapse is sufficient to show that the avalanche-size probabilities are consistent with the finite-size ansatz.

4.2 k'th Moment $\langle s^k \rangle$ Analysis

The critical components τ_s and D can also be determined numerically by measuring the k'th moment $\langle s^k \rangle$ for $k = 1, 2, 3, 4$ for the steady-state avalanche sizes, for different system sizes, shown in Figure 4.4, where:

$$\langle s^k \rangle = \lim_{T \to \infty} \frac{1}{T} \sum_{t=t_0+1}^{t_0+T} s_t^k, \tag{12}$$

and $t_0 > t_c$, the system is in steady state.

To find how the k'th moment scales with L, assuming the finite-size scaling ansatz in Eqn. (11), we approximate the k'th moment:

$$\langle s^k \rangle = \sum_{s=1}^{\infty} P(s;\, L) s^k = \sum_{s=1}^{\infty} s^k s^{-\tau_s} G(s/L^D) \propto \int_1^{\infty} s^{k-\tau_s} G(s/L^D)\, ds. \tag{13}$$

Substituting $u = \frac{s}{L^D}$, we re-write Eqn. (13)

$$\langle s^k \rangle = \int_{1/L^D}^{\infty} (uL^D)^{k-\tau_s} G(u)\, L^D\, du = L^{D(k+1-\tau_s)} \int_{1/L^D}^{\infty} (u)^{k-\tau_s} G(u) du, \tag{14}$$

where for $L \gg 1$ the lower bound approximates to zero

$$\langle s^k \rangle = L^{D(k+1-\tau_s)} \int_0^{\infty} (u)^{k-\tau_s} G(u) du. \tag{15}$$

For $u \gg 1$, $G(u)$ decays to zero, thus the integral does not diverge in the upper limit, and for $u \ll 1$, $G(0) = constant$, thus:

$$\langle s^k \rangle = L^{D(k+1-\tau_s)} G(0) \int_0^{\infty} (u)^{k-\tau_s} du, \tag{16}$$

which will not diverge in the lower limit if $k - \tau_s > -1$, or $1 + k - \tau_s > 0$. Thus,

$$\langle s^k \rangle \propto L^{D(1+k-\tau_s)},\ for\ L \gg 1,\ 1 + k - \tau_s > 0. \tag{17}$$

By plotting $\langle s^k \rangle$ against L on a double-logarithmic plot, we expect to obtain $D(1 + k - \tau_s)$ from the gradient, as shown in Figure 4.4. Figure 4.4 shows that the k'th moment scales linearly for all k in a double-logarithmic plot, and that the gradient of the straight lines increases with k as expected, demonstrating that the data is consistent with the scaling. Plotting the obtained gradients of the lines $D(1 + k - \tau_s)$ against k will enable to extract the estimates of the avalanche dimension D from the gradient and the avalanche-size exponent τ_s from the $x_{intercept}$, shown in Figure 4.5.

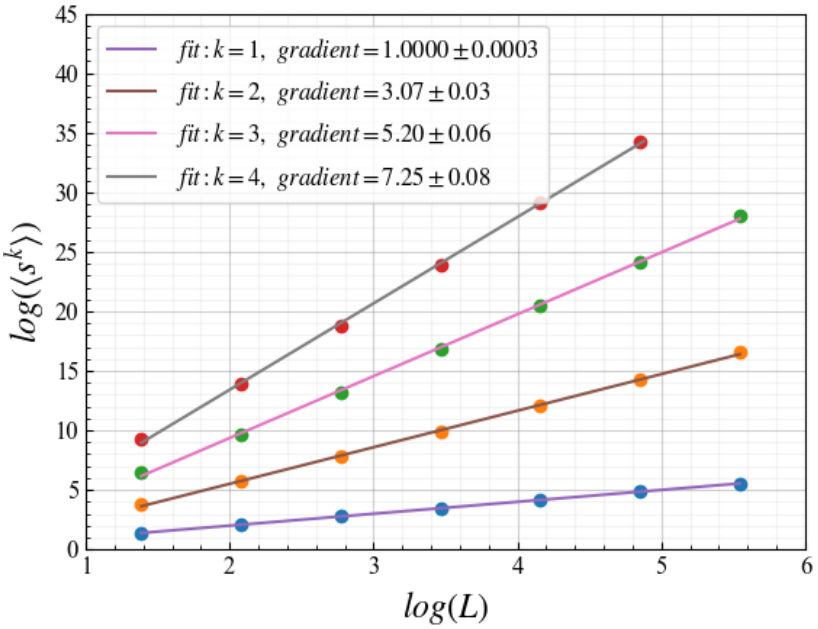

Fig. 4.4 Double-logarithmic plot of the k'th moment $\langle s^k \rangle$ against system size L, for $k = 1, 2, 3, 4$ for $L = 4, 8, 16, 32, 64, 128, 256$. A linear fit for each k has been plotted with gradients, $D(1 + k - \tau_s)$, of $1.0000 \pm 0.0002, 3.07 \pm 0.03, 5.20 \pm 0.06, 7.25 \pm 0.08$ for $k = 1, 2, 3, 4$ respectively. The straight lines of increasing gradient for increasing k are consistent with the scaling of $\langle s^k \rangle$.

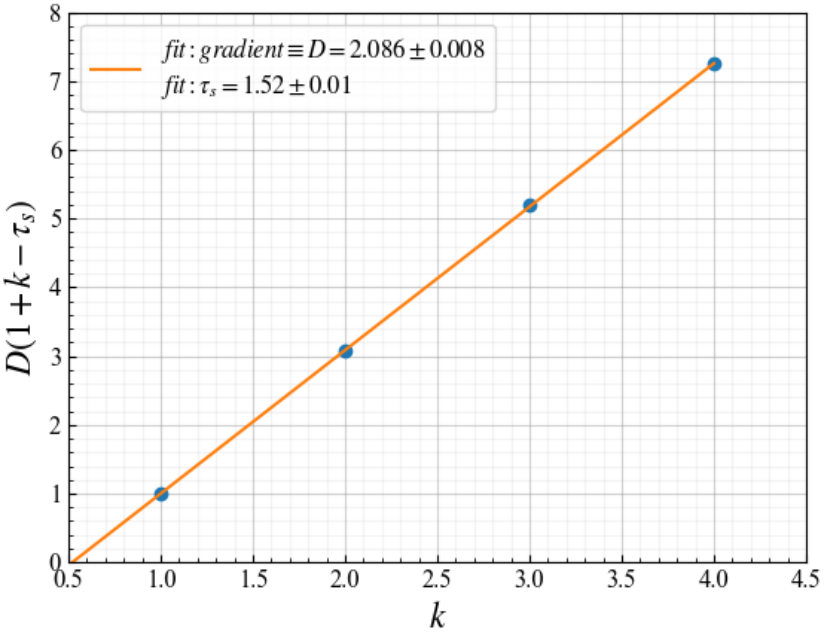

Fig. 4.5 Scaling exponent of k'th moment $D(1 + k - \tau_s)$ against k (blue dots). A linear fit (orange) with gradient of 2.086 ± 0.008, $\therefore D = 2.086 \pm 0.008$ and of $x_{intercept} = 0.52 \pm 0.01 = \tau_s - 1 \therefore \tau_s = 1.52 \pm 0.01$. The critical exponents D and τ_s are consistent with those derived from the finite-size scaling ansatz data collapse.

The critical exponents obtained are consistent with those derived from the data collapse. In addition, as the system progresses in the steady-state, $\langle grains\ added \rangle = \langle grains\ leaving \rangle$, imposing a specific scaling relation for τ_s and D, as the average

avalanche size must scale linearly with system size, $\langle s \rangle = L$. As a result, for $k = 1$ we expect $D(2 - \tau_s) = 1$. Both methods used to obtain the critical exponents are thus consistent with the scaling, as they result in $D(2 - \tau_s)$ values of 1.0128 and 1.00128 respectively, which are approximately 1.

Conclusion

The Oslo Model was successfully built, and studied to explore how it displays elements of self-organised criticality. The height of the pile was data collapsed and was investigated for scaling and signs of corrections to scaling, while the avalanche-size probability was found to be consistent with the framework for data collapse and finite-size scaling. Finally, k'th moment analysis was used to determine the critical exponents of the Oslo Model, found to be $D = 2.086 \pm 0.008$ and $\tau_s = 1.52 \pm 0.01$.

References

[1] K. Christensen, (2021), *'Complexity and Networks Course 2020-2021: Complexity Project Notes,'* Imperial College London, pg. 4,6

[2] K. Christensen; N. R. Moloney, (2020), *'Complexity & Networks: Complexity 2020-2021,'* Imperial College London, pg. 20,28

[3] M. J. Aschwanden et al., (2013), *'Self-Organized Criticality Systems,'* Open Academic Press Berlin Warsaw, pg. 38